agronomy

MDPI

Article

Improving Photosynthesis and Grain Yield in Wheat through Ridge–Furrow Ratio Optimization

Kun Liu, Yu Shi *, Zhenwen Yu, Zhen Zhang and Yongli Zhang

National Key Laboratory of Wheat Breeding, Agricultural College, Shandong Agricultural University, Tai'an 271018, China; liukun1305380@163.com (K.L.)
* Correspondence: shiyu@sdau.edu.cn

Abstract: The ridge–furrow planting pattern is an effective strategy to improve grain yield, and changes in the ridge and furrow microenvironments affect wheat yield. However, the mechanism by which wheat yields are increased at different ridge–furrow ratios is unclear. In this study, four planting modes, namely the traditional planting mode (M1) and ridge–furrow ratios of 50:50 cm (M2), 75:50 cm (M3), and 100:50 cm (M4), were established for wheat under field conditions from 2021 to 2023; the effects of different treatments on light energy utilization, dry matter accumulation and transport, and grain yield were studied. The findings demonstrated that the M3 treatment exhibited the highest enhancements in parameters such as leaf area index (LAI), canopy photosynthetically effective radiation interception rate, relative chlorophyll content (SPAD) index, and net photosynthetic rate. Moreover, the M3 treatment displayed superior grain filling compared to other treatments. The post-anthesis assimilate accumulation in the M3 treatment was 11.93%, 4.69%, and 13.13% higher than that of M1, M2, and M4 treatments, respectively, and the grain yield in M3 increased by 7.70–9.56%, 3.13–4.91%, and 8.69–10.90% compared with those in M1, M2, and M4 in the two growing seasons, respectively. In summary, under the conditions of this study, the M3 treatment led to higher LAI and SPAD values in flag leaves post-anthesis compared to the other treatments. Moreover, M3 optimized canopy structure, led to the highest canopy interception rate, and increased photosynthetic rates per individual plant. Consequently, there was a significant increase in post-anthesis dry matter accumulation, resulting in the highest grain yield achieved among the treatments.

Keywords: wheat; ridge–furrow ratio; photosynthetic characteristics; yield

Citation: Liu, K.; Shi, Y.; Yu, Z.; Zhang, Z.; Zhang, Y. Improving Photosynthesis and Grain Yield in Wheat through Ridge–Furrow Ratio Optimization. *Agronomy* **2023**, *13*, 2413. https://doi.org/10.3390/agronomy13092413

Academic Editor: Guanfu Fu

Received: 2 August 2023
Revised: 2 September 2023
Accepted: 11 September 2023
Published: 19 September 2023

1. Introduction

The Huang-Huai-Hai Plain (HHHP) is the main wheat producing area in China, accounting for 71% of the national wheat yield [1]. The development of planting patterns suitable for local production plays an important role in stabilizing and increasing wheat yield. Appropriate planting patterns can effectively improve soil structure and regulate soil fertility, thereby changing the utilization of soil water, fertilizer, gas, and heat by crops, and increasing crop yields [2,3]. However, the HHHP is one of the regions with a serious shortage of water resources, low rainfall, and large seasonal variation, which significantly impact wheat yield [4]. The ridge–furrow planting pattern is a combination of water collection and use. Many studies have shown that, compared with the traditional planting method, the ridge–furrow planting method effectively regulates soil moisture in the field by transforming the surface microtopography and saving irrigation water [5–7]. The ridge–furrow planting pattern also plays an important role in improving crop productivity and yield [8,9]. Therefore, research on the ridge–furrow planting method is of great significance for improving wheat yield in the region.

Ridge–furrow planting is a widely adopted cultivation method. In arid regions, it is established mainly in fields through ridges of various widths, using mulch to direct rainwater into ditches and minimize surface water runoff [10]. In semi-arid areas, the

broad bed–furrow method is used to optimize rainwater use and increase plant yield [11]. In waterlogging areas, the soil in the furrow is evenly covered with ridge beds, and the planting soil is lifted 2–3 cm above the saturated zone with the furrows between the ridges providing drainage runoff [12]. In irrigated areas, crops can be grown on high and low seedbeds, with irrigation only along the low seedbeds, increasing the planting area and reducing irrigation [13]. However, different ridge and furrow widths will change the plant distribution and crop yield [14], and the mechanism by which crop yield increases at different ridge–furrow ratios is unclear. Therefore, it is of great significance to explore the appropriate ridge–furrow ratio for the further improvements of such planting methods.

Crop yield mainly depends on post-anthesis material production capacities [15]. Studies have shown that canopy photosynthesis provides over 90% of the biomass for plant growth [16]. As one of the main factors affecting canopy photosynthesis, leaf photosynthesis is the main driving force for dry matter accumulation and organ formation. Canopy architecture is another major factor influencing canopy photosynthesis [17]. Liu et al. [18] found that canopy architecture is the main determinant of crop yield, because it influences light distribution and light interception. Therefore, improving the light conditions in the canopy, constructing an efficient canopy structure, and maintaining a high photosynthetic capacity of wheat in the middle and late stages of grain filling are key to increasing wheat yield.

Many studies have shown that ridge–furrow planting is a method for improving the microenvironment for crop growth, the utilization of light energy, and crop yield [19–21]. Dai et al. [22] found that the ridge–furrow planting method (ridge mulching and furrow planting) bound with supplementary irrigation and improved plant density can improve photosynthetic capacity, crop yield, and water use efficiency. Under the other ridge–furrow planting pattern (ridge planting and furrow irrigation), more incident radiation was intercepted during the key growth period, which increased the photosynthetic rates and wheat productivity [23]. Studies have found that, compared with traditional planting patterns, ridge–furrow planting patterns (ridge mulching and furrow planting) greatly improve dry matter translocation, transport efficiency, and wheat yield by improving light energy utilization [24]. Liu et al. [25] found that the ridge–furrow planting pattern of one row on the ridge and two rows in the furrow optimizes the canopy structure (i.e., longer green leaf duration and improved light transmission to lower leaf strata within the canopy) and enhances the photosynthetic capacity of single plants, thereby increasing the yield by 25.2%.

Previous studies have mainly focused on the ridge–furrow planting method to increase crop yield by co-operating with film mulching, irrigation, or planting density [22,26]; however, there are few studies on the effects of different ridge–furrow ratios on photosynthesis, crop growth, and yield formation after wheat anthesis. Therefore, the purpose of this study was to (1) analyze the effects of different ridge–furrow ratios on wheat canopy structure, photosynthetic capacity, dry matter accumulation, and yield; (2) identify the reasons for the differences in different ridge–furrow ratios; and (3) propose the optimum ridge–furrow ratio for increasing wheat yield under the experimental conditions.

2. Materials and Methods

2.1. Experimental Description and Experimental Design

Field experiments were conducted in the same field at Xiaomeng Town Experimental Station (35°40′ N, 116°24′ E) in Yanzhou District, Jining City, Shandong Province, during the growing seasons of 2021–2022 and 2022–2023. The previous crop was corn and the straw was returned to the field after harvesting. Figure 1 shows the daily mean precipitation and temperature during the wheat-growing season of this experiment. During the jointing and anthesis stages, the plants were supplemented according to an inflow of 95% (i.e., when the water reaches 95% of the treatment length, the irrigation is stopped), and the actual irrigation amount was recorded with a water meter. The well water yield of the test site was 30 $m^3 \cdot h^{-1}$, and the irrigation amount of the two growing seasons is shown in Table 1.

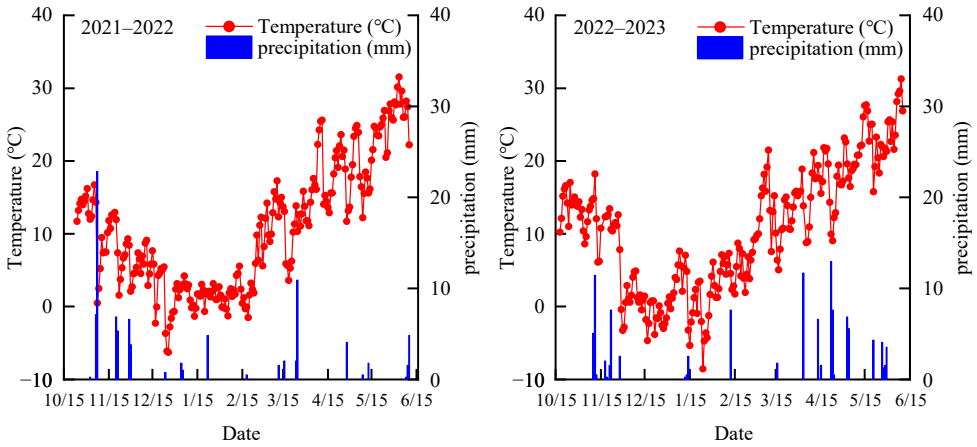

Figure 1. The daily average temperature and precipitation during the wheat-growing season in 2021–2022 and 2022–2023.

Table 1. Irrigation amount at jointing stage and anthesis stage, and total irrigation amount.

Year	Treatment	Plot Irrigation Amount		Irrigation at Jointing	Irrigation at Anthesis	Total Irrigation
		Jointing	Anthesis			
		(m^3)	(m^3)	(mm)	(mm)	(mm)
2021–2022	M1	13.57	11.31	75.4	62.83	138.23
	M2	11.63	9.56	64.6	53.1	117.7
	M3	10.37	8.16	57.6	45.34	102.94
	M4	9.09	7.16	50.51	39.78	90.29
2022–2023	M1	7.96	6.80	44.23	37.78	82.02
	M2	5.80	5.88	32.23	32.67	64.9
	M3	5.16	5.23	28.68	29.07	57.75
	M4	4.78	4.86	26.57	27	53.57

M1: Traditional planting pattern; M2: ridge–furrow planting pattern with a ridge–furrow ratio of 50:50 cm; M3: ridge–furrow planting pattern with a ridge–furrow ratio of 75:50 cm; M4: ridge–furrow planting pattern with a ridge–furrow ratio of 100:50 cm.

The wheat variety "Jimai 22" was used in this study. All plots were supplied with 240 kg·ha^{-1} N, 150 kg·ha^{-1} P (superphosphate, 42% P_2O_5), and 150 kg·ha^{-1} K (potassium chloride, 50% K_2O). All P and K fertilizers and the 105 kg·ha^{-1} N (urea, 46% N) fertilizer were applied at the sowing stage. At the jointing stage, 135 kg·ha^{-1} N (urea, 46% N) was applied. The experiment was conducted on 24 October 2021 and 18 October 2022. The planting densities were 330 plants·m^{-2} and 270 plants·m^{-2}, respectively, and were harvested on 11 June 2022 and 11 June 2023.

This study was of a randomized block design including four treatments (Figure 2): (a) M1, traditional planting pattern; (b) M2, ridge–furrow planting pattern with a ridge–furrow ratio of 50:50 cm; (c) M3, ridge–furrow planting pattern with a ridge–furrow ratio of 75:50 cm; and (d) M4, ridge–furrow planting pattern with a ridge–furrow ratio of 100:50 cm. Each treatment was replicated three times, each plot was 30 m long and 6 m wide, and the area was 180 m^2. The experimental soil was as follows: organic matter, 14.79 g·kg^{-1}; total nitrogen, 1.23 g·kg^{-1}; available nitrogen, 120.3 mg·kg^{-1}; available phosphorus, 30.86 mg·kg^{-1}; and available potassium, 119.6 mg·kg^{-1}. Pesticides and herbicides were applied according to normal practices.

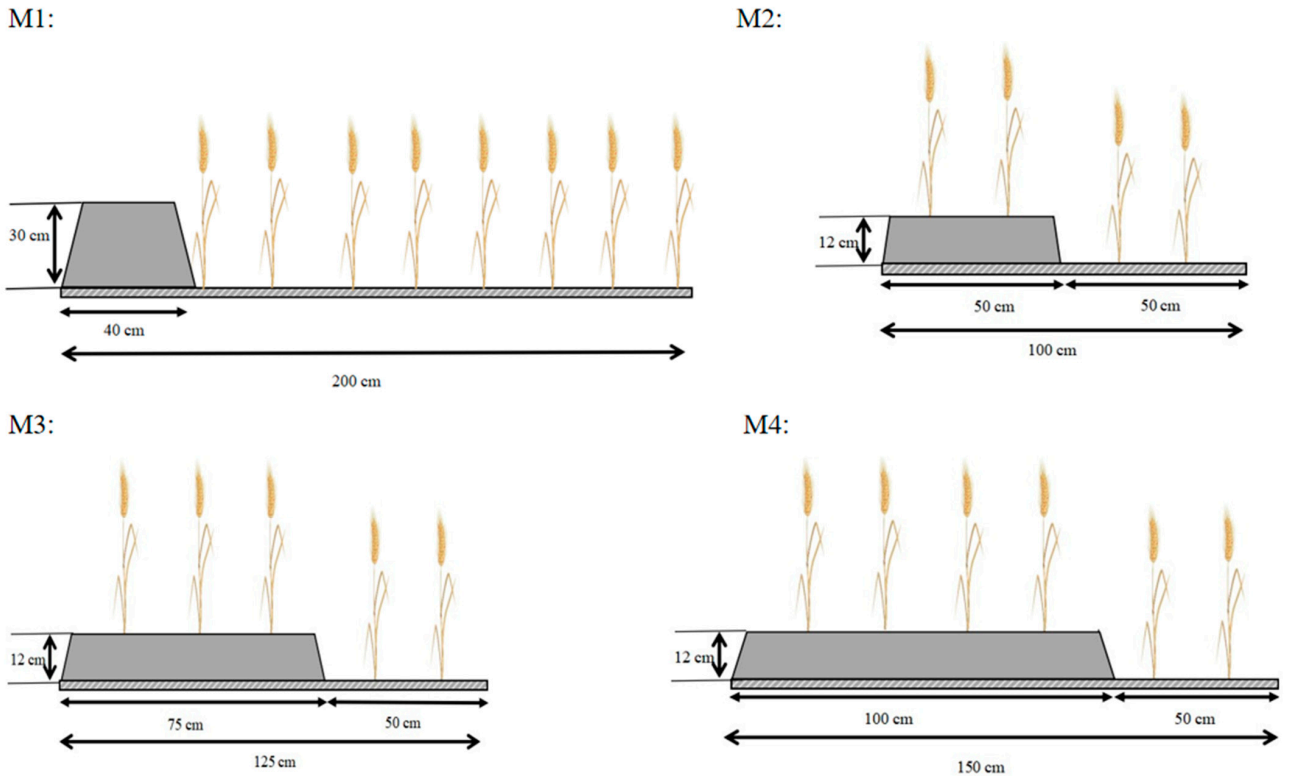

Figure 2. Planting pattern diagram. M1: Traditional planting pattern; M2: ridge–furrow planting pattern with a ridge–furrow ratio of 50:50 cm; M3: ridge–furrow planting pattern with a ridge–furrow ratio of 75:50 cm; M4: ridge–furrow planting pattern with a ridge–furrow ratio of 100:50 cm.

2.2. Grain Yield Determination

Following the protocol described by Si et al. [27], sampling was performed with each row according to the traditional planting pattern, and in the ridge–furrow planting pattern. Samples were taken for each row on the ridge and furrow, respectively. At the physiological maturity stage, all rows of wheat with a length of 4 m from each plot were harvested, and grains were naturally air-dried at 13% water content, weighed, and converted into the final yield by weighted average. In each plot, the number of spikes was determined in a 1 m row and calculated using the weighted average. Forty plants from each plot were randomly collected to measure the kernels per spike. A total of 1000 seeds were randomly collected from the yield test samples and weighed, and the 1000-grain weight was calculated. All treatments were repeated three times.

2.3. Leaf Area Index (LAI)

The leaf area was measured at anthesis and at 7, 4, 21, and 28 days after anthesis, according to Han et al. [28]. Twenty representative wheat plants were randomly selected at each treatment, and all treatments were repeated three times. The length and width of all fully spread green leaves were measured, and the leaf area was calculated and averaged. The formula for calculating LAI is as follows:

$$LAI = 0.83 \times \rho \times \sum_{i=1}^{n} (a_i \times b_i) \quad (1)$$

where ρ is the total number of stems per unit area of wheat, 0.83 is the correction coefficient, a and b are the length and maximum leaf width of wheat leaves, and i is the number of leaves.

2.4. Relative Chlorophyll Content (SPAD) of Flag Leaf

The SPAD was determined at anthesis and at 7, 14, 21, and 28 d after anthesis (9:30–11:30 a.m.). In the absence of wind and sunny weather, 20 flag leaves with consistent growth were selected from each row for each treatment and measured using a chlorophyll meter (CCM-200, Tyngsboro, MA, USA). All treatments were repeated three times.

2.5. Canopy Light Interception Efficiency (In) and Transmittance (LT)

The SunScan canopy instrument (Delta-T Devices SunScan, Cambridge, UK) was used to measure the transmission and incident radiation to the ground, similarly to Shahzad et al. [19]. The experiment was carried out at 9:30–11:30 a.m. on five sunny days of wheat anthesis and at 7, 14, 21, and 28 days after anthesis. A canopy analyzer was placed parallel to the row direction near the root of each row of wheat in each plot to measure the transmitted radiation. The means of these measurements were considered as canopy-transmitted radiation. The photosynthetically active radiation (PAR) interception efficiency (In) and canopy transmittance (LT) were calculated as follows:

$$\text{In } (\%) = (1 - \text{PAR}_i/\text{TPAR}) \times 100 \quad (2)$$

$$\text{LT } (\%) = (\text{PAR}_i/\text{TPAR}) \times 100 \quad (3)$$

where TPAR is the incident PAR at the top of the canopy, and PAR_i is the ground incident PAR near the root zone of wheat.

2.6. Photosynthetic Parameters of The Flag Leaf

The net photosynthetic rate (P_n), stomatal conductance (G_s), transpiration rate (T_r), and intercellular CO_2 concentration (C_i) of the flag leaves were measured using an LI-6400XT photosynthesis apparatus (LI-COR, Lincoln, NE, USA) under natural light conditions in the field [29]. The fully expanded flag leaves were measured at 9:00–11:00 a.m. on sunny days. The photosynthetically active radiation was set to 1500 μmol m^{-2} s^{-1} and the light source was a red-blue light source. The vapor pressure deficit (VPD) was set to 1500 kPa, and the leaf temperature was stable at 25 ± 1 °C. The reference and sample gas analyzer signals were matched before logging the data. At anthesis and at 7, 14, 21, and 28 days after anthesis, three replicates were taken from each treatment, and the average value of 9 leaves were taken for each replicate for analysis. The ridge–furrow planting pattern was measured on the ridge and in the furrow, respectively.

2.7. Dry Matter Accumulation and Translocation

Sampling was performed according to Fan et al. [30] from each row in the traditional planting pattern; in the ridge–furrow planting pattern, samples were taken each row on the ridge and furrow, respectively. Samples were collected at the anthesis and maturity stages of wheat, and 20 single stems were randomly selected from each row for each treatment and analyzed three times. The anthesis period was divided into three parts: stem + sheath, leaf, and spike. The maturation period was divided into four parts: stem + leaf sheath, leaf, cob + glume, and grain. The plants were placed in an oven at 105 °C for 30 min and dried at 80 °C. The dry matter weight was determined. The transport and accumulation of assimilates were calculated as follows:

$$\begin{gathered}\text{Amount of dry matter transferred to vegetative organs } (\text{kg}\cdot\text{ha}^{-1}) = \text{amount} \\ \text{of dry matter in vegetative organs at the anthesis} - \text{amount of dry matter in} \\ \text{vegetative organs at the maturity}\end{gathered} \quad (4)$$

$$\begin{gathered}\text{Contribution rate of vegetative organ dry matter } (\%) = (\text{amount of dry} \\ \text{matter transferred to vegetative organs/amount of dry matter in the grains} \\ \text{at maturity}) \times 100\end{gathered} \quad (5)$$

$$\text{Amount of dry matter accumulated after anthesis (kg·ha}^{-1}\text{)} = \text{amount of dry matter in the grains at the maturity} - \text{amount of transferred dry matter of vegetative organs} \quad (6)$$

$$\text{Contribution rate of dry matter accumulated after anthesis to grains (\%)} = (\text{amount of dry matter accumulated in grains after anthesis/amount of dry matter in the grains at the maturity}) \times 100 \quad (7)$$

2.8. Data Analysis

The experimental data for each growing season were analyzed via ANOVA using IBM SPSS Statistics 26.0 (IBM Corp, Armonk, NY, USA). The Degrees of Freedom (df) in the ANOVA was two. Significant differences of the mean values among treatments were evaluated using the least significant differences (LSD) test at $p < 0.05$. All experimental results were the averages of three replications. Figures were drawn using Origin 2021 (Origin Lab, Northampton, MA, USA). The values used for photosynthetic parameters, dry matter accumulation, and the distribution of flag leaves after anthesis were the average for the 2021–2022 and 2022–2023 periods. The ridge–furrow planting patterns were calculated using the weighted average method [31].

3. Results

3.1. Yield and Yield Components

Significant differences in grain yield were observed among the different planting patterns ($p < 0.05$) (Table 2). In the growing seasons of 2021–2022 and 2021–2022, the grain yield of M3 was significantly higher than that of other treatments ($p < 0.05$). The grain yield of M3 for the two years increased by 7.70% and 9.56%, respectively, compared to that of M1. The grain yield in M2 increased by 4.44% and 4.55%, respectively. However, the grain yield of M4 did not improve. The grain yield in the M3 ridge was significantly higher than that in the M4 ridge and M1 in both growing seasons, and was higher than that of the M2 ridge in 2022–2023 ($p < 0.05$). However, there was no significant difference in grain yield between the M3 and M2 ridges from 2021 to 2022 ($p < 0.05$). The grain yield in the M3 and M4 furrows was significantly higher than that in the M2 furrow and M1 in both growing seasons ($p < 0.05$). The effect of the M3 treatment on wheat grain yield was more significant ($p < 0.05$). The yield components also varied with the treatment. The results of this study showed that each treatment had significant effects on the 1000-grain weight and spike number ($p < 0.05$), which were significantly higher in the M3 treatment than those in the other treatments ($p < 0.05$). The difference in kernel number per spike was not significant ($p < 0.05$).

Table 2. Wheat yield and its components under different treatments.

Year	Treatment		Spike Number (10^4·ha^{-1})	Mean	Kernel Number per Spike	Mean	Thousand Kernel Weight (g)	Mean	Yield (kg·ha^{-1})	Mean
2021–2022	M1	-	657.9 c	657.9 b	36.91 bc	36.91 a	44.38 d	44.38 c	9101 b	9101 c
	M2	ridge	654.6 c	658.6 b	37.30 ab	37.35 a	47.46 b	45.68 b	9813 a	9505 b
		furrow	662.6 c		37.40 ab		43.89 d		9197 b	
	M3	ridge	663.5 c	675.2 a	36.23 c	37.19 a	48.50 a	45.99 a	9851 a	9802 a
		furrow	692.7 b		38.23 a		43.53 d		9730 a	
	M4	ridge	605.2 d	642.6 c	36.70 bc	36.50 a	45.44 c	45.74 c	8644 c	9019 c
		furrow	717.5 a		38.11 a		42.33 e		9769 a	

Table 2. *Cont.*

Year	Treatment		Spike Number ($10^4 \cdot ha^{-1}$)	Mean	Kernel Number per Spike	Mean	Thousand Kernel Weight (g)	Mean	Yield ($kg \cdot ha^{-1}$)	Mean
2022–2023	M1	-	612.1 bc	612.1 b	40.20 a	40.20 a	40.45 d	40.45 c	8538 c	8538 c
	M2	ridge	604.9 c	614.9 b	40.64 a	40.23 a	44.05 b	42.10 b	9270 b	8927 b
		furrow	624.9 b		39.81 a		40.15 d		8584 c	
	M3	ridge	613.4 bc	631.5 a	40.24 a	39.90 a	46.12 a	43.59 a	9707 a	9355 a
		furrow	658.7 a		39.40 a		39.80 d		8827 b	
	M4	ridge	548.4 d	588.4 c	39.84 a	39.67 a	43.12 c	42.05 b	8148 d	8435 c
		furrow	668.4 a		39.32 a		39.90 d		9009 b	

Different lowercase letters indicated a significant difference at the $p < 0.05$ level in the same year (LSD test). M1: Traditional planting pattern; M2: ridge–furrow planting pattern with a ridge–furrow ratio of 50:50 cm; M3: ridge–furrow planting pattern with a ridge–furrow ratio of 75:50 cm; M4: ridge–furrow planting pattern with a ridge–furrow ratio of 100:50 cm.

3.2. LAI

The wheat post-anthesis LAI was significantly affected by different ridge–furrow planting patterns ($p < 0.05$) (Table 3). The average LAI of the M3 treatment after anthesis in the two growing seasons was 6.87–12.72%, 3.55–6.69%, and 7.00–12.81% higher than those in the M1, M2, and M4 treatments, respectively, and the difference was more obvious with the filling process ($p < 0.05$). The LAI changes in the ridge and furrow were similar in the two years, and the LAI in the furrow of the ridge–furrow planting pattern was significantly higher than that in M1 after wheat anthesis ($p < 0.05$). In the ridge–furrow planting pattern, the LAI on the ridge was significantly higher in the M3, M2 ridges, and M1 than that on the M4 ridge at anthesis ($p < 0.05$). The LAI for each treatment at 7–28 d after anthesis followed the order M3 ridge > M2 ridge = M1 > M4 ridge. The results showed that the M3 treatment significantly regulated the LAI of the wheat, ensuring a high photosynthetic area after anthesis, and laying the foundations for a high crop yield.

Table 3. Leaf area index of wheat after anthesis under different treatments.

Year	Treatment		Days after Anthesis									
			0	Mean	7	Mean	14	Mean	21	Mean	28	Mean
2021–2022	M1	-	6.14 c	6.14 b	5.75 c	5.75 c	5.13 d	5.13 c	3.38 d	3.38 c	2.35 c	2.25 c
	M2	ridge	6.15 c	6.30 a	5.84 c	6.06 b	5.24 d	5.54 b	3.53 c	3.54 b	2.33 c	2.49 b
		furrow	6.44 b		6.27 a		5.84 b		3.54 c		2.65 b	
	M3	ridge	6.18 c	6.34 a	6.02 b	6.16 a	5.66 c	5.98 a	3.62 c	3.97 a	2.60 b	3.08 a
		furrow	6.59 ab		6.36 a		6.15 a		4.04 b		3.21 a	
	M4	ridge	5.88 d	6.16 b	5.56 d	5.82 c	4.62 e	5.08 c	2.74 e	3.37 c	1.72 d	2.20 d
		furrow	6.72 a		6.33 a		6.01 a		4.42 a		3.15 a	
2022–2023	M1	-	6.18 b	6.18 a	5.82 d	5.82 b	5.23 d	5.23 c	4.24 d	4.24 c	2.84 c	2.84 c
	M2	ridge	6.20 b	6.31 a	5.87 d	6.04 a	5.22 d	5.40 b	4.21 d	4.37 b	2.81 c	2.97 b
		furrow	6.41 b		6.21 b		5.57 c		4.52 c		3.12 b	
	M3	ridge	6.26 b	6.41 a	6.05 c	6.19 a	5.43 c	5.62 a	4.40 c	4.60 a	3.07 b	3.16 a
		furrow	6.64 a		6.41 a		5.90 b		4.90 b		3.30 a	
	M4	ridge	5.93 c	6.18 a	5.48 e	5.83 b	4.77 e	5.22 c	3.78 e	4.22 c	2.61 d	2.83 c
		furrow	6.67 a		6.54 a		6.13 a		5.11 a		3.28 a	

Different lowercase letters indicated a significant difference at the $p < 0.05$ level in the same year (LSD test). M1: Traditional planting pattern; M2: ridge–furrow planting pattern with a ridge–furrow ratio of 50:50 cm; M3: ridge–furrow planting pattern with a ridge–furrow ratio of 75:50 cm; M4: ridge–furrow planting pattern with a ridge–furrow ratio of 100:50 cm.

3.3. Flag Leaf SPAD Index

The ridge–furrow planting patterns had a significant effect on the SPAD index ($p < 0.05$) (Figure 3A–D). From 0 to 14 d after anthesis, no significant difference was observed in the SPAD index of flag leaves between the M2 and M3 treatments for the two years, but it was significantly higher than that of the M1 and M4 treatments ($p < 0.05$). Compared with M2, M1, and M4 treatments, the SPAD in the M3 treatment increased by 5.05–7.34%, 9.52–14.13%, and 9.94–15.50%, respectively, from 21 to 28 d after anthesis. The M3 treatment was superior to the other treatments because, in the growing seasons of 2021–2022 and 2022–2023, the SPAD index on the ridge in the M3 treatment was significantly higher than that of the other treatments from 7 to 28 d after anthesis ($p < 0.05$). The SPAD index in the furrow of the M3 treatment was significantly higher than that in the M1, M2, and M4 treatments 21–28 d after anthesis ($p < 0.05$). The results showed that the M3 treatment increased the SPAD index of flag leaves in the late anthesis stage of wheat, prolonging the green leaf time, and improving the photosynthetic capacity.

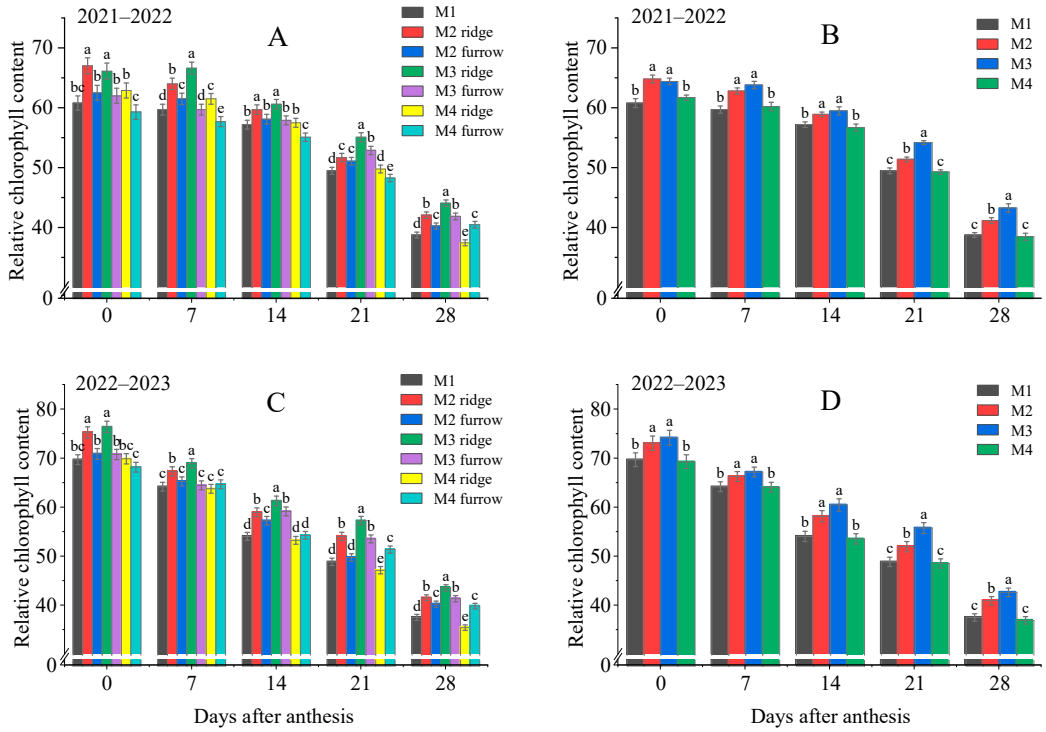

Figure 3. SPAD (**A**–**D**) of wheat flag leaf after anthesis under different treatments. Different lowercase letters indicate a significant difference at the $p < 0.05$ level in the same year (LSD test). M1: Traditional planting pattern; M2: ridge–furrow planting pattern with a ridge–furrow ratio of 50:50 cm; M3: ridge–furrow planting pattern with a ridge–furrow ratio of 75:50 cm; M4: ridge–furrow planting pattern with a ridge–furrow ratio of 100:50 cm.

3.4. Canopy PAR In and LT

The PAR In of the wheat after anthesis showed a decreasing trend in both growing seasons (Figure 4A,C), whereas canopy PAR LT transmittance showed an increasing trend (Figure 4B,D). The decrease in canopy PAR in the M3 treatment was the smallest in the middle and late stages of wheat growth after anthesis, and it was significantly higher than that of the other treatments from 14 to 28 d after anthesis ($p < 0.05$). The post-anthesis wheat canopy LT was the highest in the M4 and M1 treatments in both years, followed by the M2 treatment, and the M3 treatment was the lowest. The M3 treatment decreased by 6.38–33.88% compared with other treatments. The M3 treatment significantly increased the In of the canopy PAR and improved the utilization of light energy.

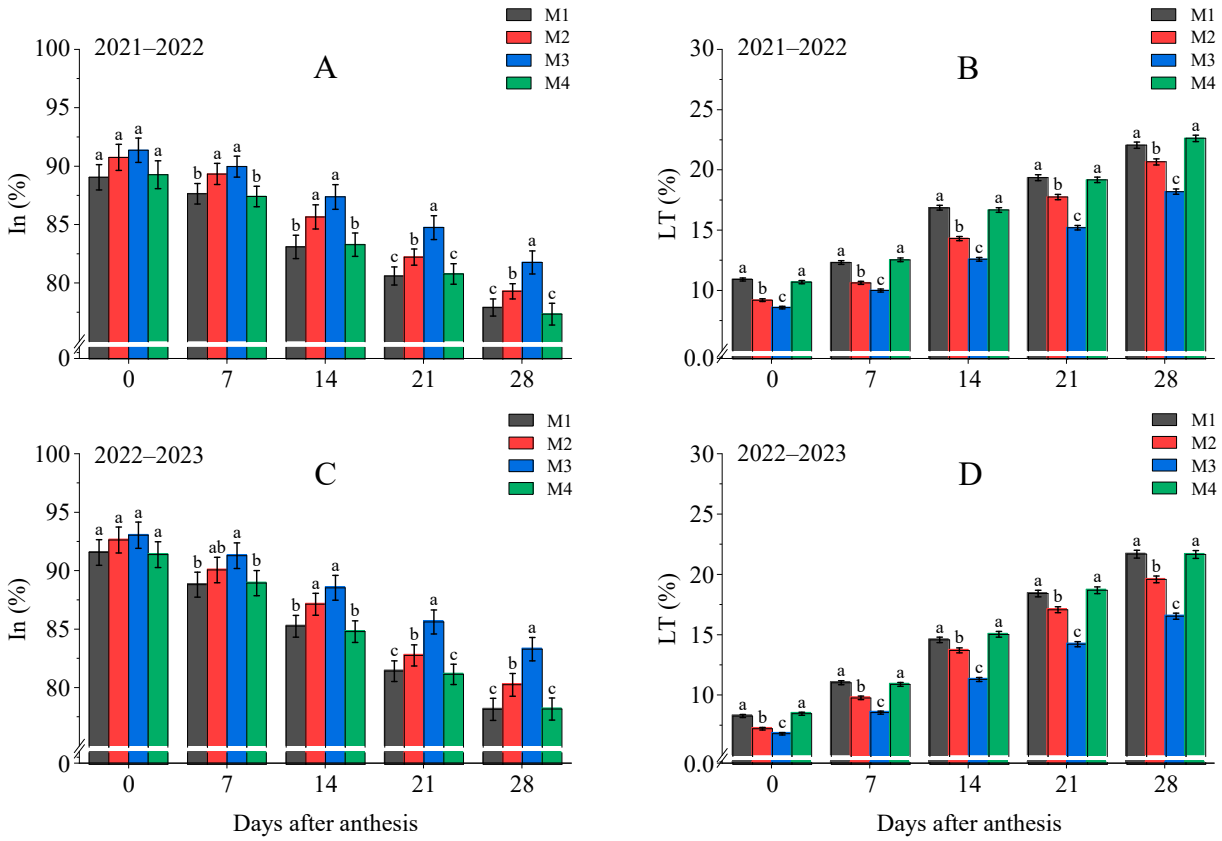

Figure 4. Canopy photosynthetically active radiation interception rate (**A**,**C**) and transmittance (**B**,**D**) of wheat after anthesis under different treatments. Different lowercase letters indicate a significant difference at the $p < 0.05$ level in the same year (LSD test). M1: Traditional planting pattern; M2: ridge–furrow planting pattern with a ridge–furrow ratio of 50:50 cm; M3: ridge–furrow planting pattern with a ridge–furrow ratio of 75:50 cm; M4: ridge–furrow planting pattern with a ridge–furrow ratio of 100:50 cm.

3.5. Photosynthetic Parameters of Flag Leaves

The photosynthetic indices for the different treatments first increased and then decreased. The photosynthetic indexes reached a maximum at 7 d after anthesis (Figure 5A–H). No significant differences in photosynthetic indices were observed among the different treatments at the anthesis stage ($p < 0.05$). From 7 to 28 d after anthesis, the photosynthetic indexes were the highest in the M3 treatment, followed by those in the M2 treatment, and were the lowest in the M1 and M4 treatments (Figure 5B,D,F,H). The photosynthetic indices on the ridge in the M3 treatment were significantly higher than those in the other treatments after wheat anthesis ($p < 0.05$). The photosynthetic indices in the furrow of the ridge–furrow planting pattern showed that the photosynthetic indices were significantly higher in M3 than those in the M2, M4, and M1 treatments 21–28 days after anthesis ($p < 0.05$). The net photosynthetic rate of the M3 treatment was 9.08–63.29% higher than that of other treatments at 14–28 days after wheat anthesis. This indicates that the M3 treatment was beneficial for improving the photosynthetic capacity of wheat, thereby improving the crop production capacity of the crop.

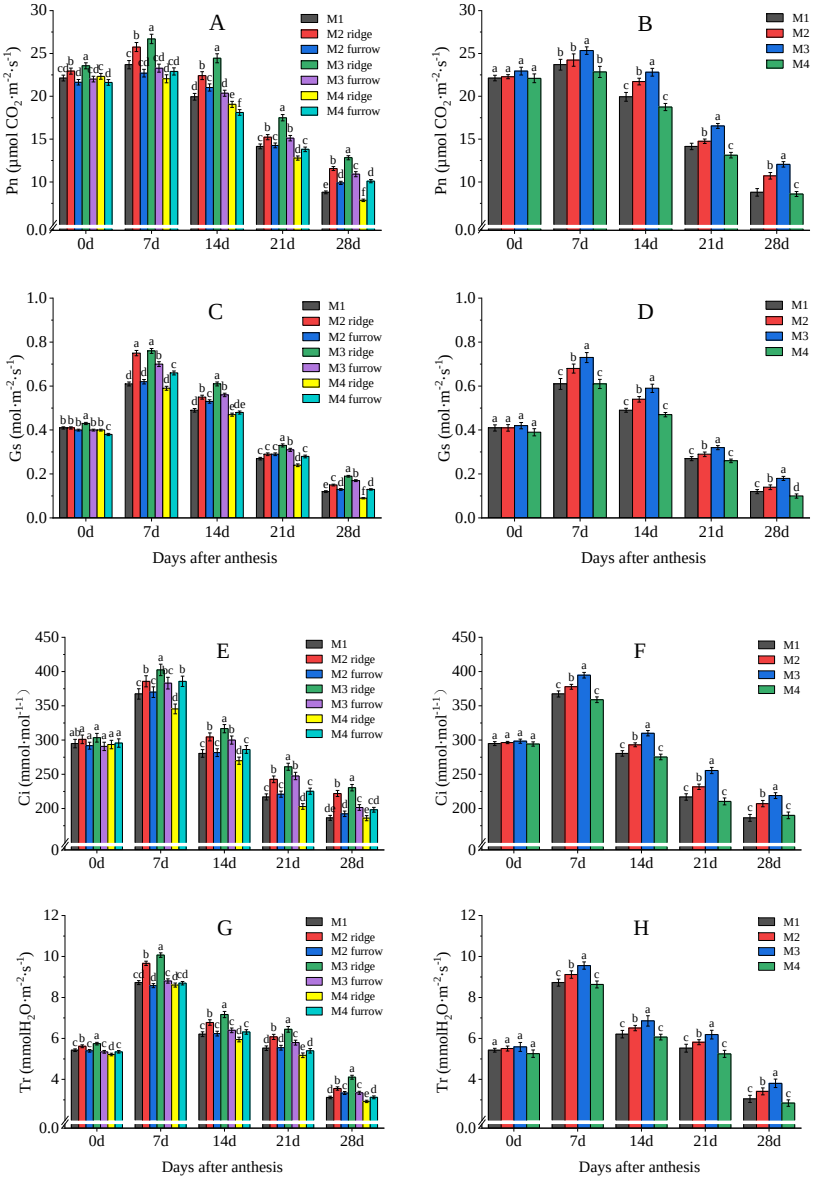

Figure 5. Photosynthetic parameters (**A**–**H**) of wheat flag leaves after anthesis under different treatments. The values are given from two average years, and different lowercase letters on the column indicate significant differences at the $p < 0.05$ levels (LSD test). M1: Traditional planting pattern; M2: ridge–furrow planting pattern with a ridge–furrow ratio of 50:50 cm; M3: ridge–furrow planting pattern with a ridge–furrow ratio of 75:50 cm; M4: ridge–furrow planting pattern with a ridge–furrow ratio of 100:50 cm.

3.6. Accumulation and Translocation of Dry Matter at Pre- and Post-Anthesis Period

The ridge-furrow planting pattern had a significant effect on dry matter accumulation and transport after anthesis ($p < 0.05$) (Table 4). Compared with the traditional planting pattern, M3 significantly increased dry matter accumulation at the mature stage ($p < 0.05$), whereas the dry matter accumulation in M2 was not significantly different from that in M1 ($p < 0.05$). The dry matter accumulation in M4 was even lower than that of the traditional planting pattern. No significant difference was observed in the transport of dry matter stored in the vegetative organs before anthesis ($p < 0.05$). The accumulation of assimilates after anthesis in the ridge and furrow of the M3 treatment was higher than that of the M1, M2, and M4 treatments. The accumulation of assimilates after anthesis in the M3 treatment was 11.92%, 4.68%, and 13.12% higher than that in M1, M2, and M4 treatments, respectively.

Table 4. Accumulation and translocation of dry matter at pre- and post-anthesis period under different treatments.

Treatment		Anthesis (kg·ha^{-1})	Mean	Maturity (kg·ha^{-1})	Mean	Pre-Anthesis Storage of Assimilates				Post-Anthesis Assimilates			
						Translocation (kg·ha^{-1})	Mean	Contribution Rate to Grain (%)	Mean	Accumulation (kg·ha^{-1})	Mean	Contribution Rate to Grain (%)	Mean
M1	-	13,085 c	13,085 a	19,218 a	19,218 b	2702 c	2702 a	30.60 b	30.60 a	6133 d	6133 c	69.40 c	69.40 b
M2	ridge	12,621 c	12,829 a	19,312 c	19,385 b	3044 a	2764 a	31.27 a	29.59 b	6691 b	6557 b	68.73 c	70.41 ab
	furrow	13,036 c		19,458 c		2484 d		27.90 d		6422 c		72.10 ab	
M3	ridge	12,740 c	13,139 a	19,596 c	20,003 a	2904 b	2721 a	29.76 c	28.35 c	6856 a	6864 a	70.24 bc	71.65 a
	furrow	13,737 b		20,614 b		2447 d		26.25 e		6876 a		73.75 a	
M4	ridge	11,384 d	12,444 b	17,148 d	18,511 c	2669 c	2691 a	31.68 a	30.81 a	5763 e	6068 c	68.32 c	69.19 b
	furrow	14,562 a		21,238 a		2734 c		29.07 c		6676 b		70.93 bc	

The values are given from two average years, and different lowercase letters indicate significant differences at $p < 0.05$ levels in the same line (LSD test). M1: Traditional planting pattern; M2: ridge–furrow planting pattern with a ridge–furrow ratio of 50:50 cm; M3: ridge–furrow planting pattern with a ridge–furrow ratio of 75:50 cm; M4: ridge–furrow planting pattern with a ridge–furrow ratio of 100:50 cm.

4. Discussion

4.1. Crop Yield and Yield Components

The ridge–furrow planting pattern had a significant influence on wheat yield. Studies have shown that ridge–furrow planting patterns can effectively promote crop development and increase grain yield [32,33]. The increase in crop yield is affected by the proportion of ridges and furrows. In the present study, the crop yield increased with an increase in the ridge–furrow ratio within a certain range and did not increase significantly after exceeding a certain proportion [34,35]. With the increase in the ridge–furrow ratio, the wheat yield reached a maximum in the M3 treatment (ridge–furrow ratio 75:50 cm) and then decreased. One aspect of this is related to the fact that a higher ridge–furrow ratio enhances rainwater collection and reduces irrigation water loss. As a result, this delays the senescence of wheat in the furrow and ensures that sufficient water is provided for wheat plants on the ridge. On the other hand, a too-high ridge–furrow ratio results in insufficient water supply for ridge-based wheat plants, resulting in negative effects, affecting the earing and filling of wheat plants on the ridge (Table 2), and reducing wheat yield.

4.2. Canopy Development and Light Energy Capture

Canopy structure is an important factor affecting light distribution and energy capture. Improving the ability to capture light energy is a most important strategy for increasing crop yield [36]. In this study, the Leaf Area Index (LAI) after anthesis in plants under the M3 treatment exhibited superior results compared to the other treatments. This disparity was particularly pronounced during the grain filling phase. The canopy PAR In showed the same pattern. The reason for the predominance of M3's post-anthesis LAI and canopy PAR In may be that a higher ridge–furrow ratio can promote the growth and development of wheat in the trench [37], thereby maintaining the highest LAI in the effective filling period (Table 3), which is conducive to reducing light leakage loss and resulting in higher light energy effective interception, whereas the canopy PAR In is greatly reduced in M4 because of the greatly reduced ridge LAI. Therefore, an appropriate ridge–furrow ratio is beneficial for improving the LAI, delaying leaf aging, and improving light energy utilization [14,38], thereby improving canopy structure, increasing photosynthetically effective radiation interception, enhancing photosynthetic assimilation, ensuring sufficient nutrient supply during grain filling, and providing a material basis for increasing wheat yield.

4.3. Photosynthetic Characteristics

Light is essential for plant growth and development, and the leaf photosynthetic capacity reflects the growth status of winter wheat and determines crop productivity. Suitable planting patterns not only increase leaf areas, but also extend photosynthetic time, thereby improving photosynthetic capacity [21]. This study found that ridge–furrow planting had the advantage of improving the photosynthetic capacity of crop leaves [39,40]. However, this study showed that, compared with the M1 treatment, the M3 and M2 treatments increased the SPAD index and net photosynthetic rate, while that of the M4 treatment with the highest ridge–furrow ratio did not increase or even decreased. The increase in the net photosynthetic rate in the M3 and M2 treatments may be related to the improvement in the photosynthetic index by changing the microtopography and the difference in the vertical height of neighboring ridges and furrows. This changes individual niches, affecting the competitiveness of plant light resources, and improving the photosynthetic index [41], especially in the late stage of wheat growth when there is fierce competition for nutrition, light, and water between individual plants [17]. However, the M4 treatment ridge was too wide, resulting in uneven water distribution after irrigation, insufficient water on the ridge, stomatal closure, a reduced photosynthesis rate, and decreased chlorophyll content, inducing oxidative stress, accelerating aging, and reducing the life of the functional leaves [42].

4.4. Dry Matter Accumulation and Translocation

Wheat yield is composed of the transport of the dry matter stored before anthesis to grain and the accumulation of dry matter after anthesis. Studies have shown that ridge–furrow planting can promote the synthesis of dry matter and its transfer from the vegetative to reproductive organs, thereby increasing grain yield [43,44]. An appropriate increase in the ridge width can promote the accumulation of wheat assimilates, which is beneficial for dry matter accumulation after anthesis [34]. This study found that the M3 treatment with wider ridges had the largest dry matter production after wheat anthesis, and the dry matter transport after anthesis was higher than that in the M1 treatment, whereas the dry matter production and transport in the M4 treatment with the widest ridges was not significantly different from those in M1. This is mainly because suitable ridge and furrow planting can optimize the utilization of light energy by crops. The transformation from flat light to three-dimensional light significantly increases the light-receiving area and time of crops, results in the hierarchical and three-dimensional utilization of light by crops, and makes the accumulation of dry matter in crops easier [10]. In addition, this study found that with an increase in the ridge–furrow ratio at maturity, the dry matter accumulation of wheat in the furrows in M2, M3, and M4 increased compared to that in M1. However, the increase in dry matter accumulation on the wheat ridges was not notable, and decreased in the M4 ridges. Therefore, with an increase in ridge width, the accumulation of wheat dry matter in the furrow can increase to some extent [45]. In contrast, a wider ridge can further reduce the use of irrigation water, but too little water will make the wheat water supply on the ridge insufficient, causing drought stress to the wheat and leading to the premature aging of wheat; this will reduce the accumulation time of photosynthetic substances on the ridges of wheat, which is not conducive to the accumulation of assimilates after anthesis [46]. Therefore, choosing the correct ridge–furrow ratio is crucial for crop growth and development.

5. Conclusions

In this study, we show that the photosynthetic characteristics and wheat yield after anthesis are closely related to the planting method. The ridge–furrow planting mode with a ridge–furrow ratio of 75:50 cm had the highest grain yield. This was primarily attributed to the optimization of the canopy structure after wheat anthesis, including an enhanced LAI and canopy PAR In. Additionally, improvements in photosynthetic performance, such as an increased net photosynthetic rate and SPAD index, played a significant role. These enhancements led to better CO_2 assimilation at physiological maturity, and consequently, higher grain yield. While the effects of the ridge–furrow ratio on wheat quality need to be further investigated, these results suggest that the ridge–furrow planting method with a ratio of 75:50 cm is suitable for the winter wheat production in the Huang-Huai-Hai region.

Author Contributions: K.L.: conceptualization; investigation; data curation; writing—original draft, and review and editing. Y.S.: conceptualization; funding acquired; and writing–review and editing. Z.Y.: conceptualization. Z.Z.: writing–review and editing. Y.Z.: supervision. All authors have read and agreed to the published version of the manuscript.

Funding: This study was financially supported by the National Natural Science Foundation of China (32172114); the China Agriculture Research System of MOF and MARA (CARS-03-18); and the Taishan Scholar Project Special Funds.

Data Availability Statement: The data of this study can be obtained from the corresponding author.

Acknowledgments: The authors would like to thank the reviewers for their valuable comments and suggestions for this work.

Conflicts of Interest: The authors declare no conflict of interest.

References

1. Xu, X.X.; Liu, S.; Meng, F.G.; Zhang, X.; Zhao, J.K.; Qu, W.K.; Shi, Y.; Zhao, C.X. Grain yield formation and nitrogen utilization efficiency of different winter wheat varieties under rainfed conditions in the Huang-Huai-Hai Plain. *Agronomy* **2023**, *13*, 915. [CrossRef]
2. Zhang, J.J.; Mu, J.Y.; Hu, Y.A.; Ren, A.X.; Lei, B.; Ding, P.C.; Li, L.H.; Sun, M.; Gao, Z.Q. Effect of Planting Patterns and Seeding Rate on Dryland Wheat Yield Formation and Water Use Efficiency on the Loess Plateau, China. *Agronomy* **2023**, *13*, 851. [CrossRef]
3. Wu, F.Q.; Qiu, Y.R.; Huang, W.B.; Guo, S.M.; Han, Y.C.; Wang, G.P.; Li, X.F.; Lei, Y.P.; Yang, B.F.; Xiong, S.W.; et al. Water and heat resource utilization of cotton under different cropping patterns and their effects on crop biomass and yield formation. *Agric. For. Meteorol.* **2022**, *323*, 109091. [CrossRef]
4. Ren, P.P.; Huang, F.; Li, B.G. Spatiotemporal patterns of water consumption and irrigation requirements of wheat-maize in the Huang-Huai-Hai Plain, China and options of their reduction. *Agric. Water Manag.* **2022**, *263*, 107468. [CrossRef]
5. Gu, X.B.; Cai, H.J.; Chen, P.P.; Li, Y.P.; Fang, H.; Li, Y.N. Ridge-furrow film mulching improves water and nitrogen use efficiencies under reduced irrigation and nitrogen applications in wheat field. *Field Crops Res.* **2021**, *270*, 108214. [CrossRef]
6. Zhang, Y.Y.; Zhao, X.N.; Wu, P.T. Soil Wetting Patterns and Water Distribution as Affected by Irrigation for Uncropped Ridges and Furrows. *Pedosphere* **2015**, *25*, 468–477. [CrossRef]
7. Si, Z.Y.; Qin, A.Z.; Liang, Y.P.; Duan, A.W.; Gao, Y. A review on regulation of irrigation management on wheat physiology, grain yield, and quality. *Plants* **2023**, *12*, 692. [CrossRef]
8. Fang, H.; Li, Y.N.; Gu, X.B.; Li, Y.P.; Chen, P.P. Can ridge-furrow with film and straw mulching improve wheat-maize system productivity and maintain soil fertility on the Loess Plateau of China? *Agric. Water Manag.* **2021**, *246*, 106686. [CrossRef]
9. Liu, Y.; Zhang, X.L.; Xi, L.Y.; Liao, Y.C.; Han, J. Ridge-furrow planting promotes wheat grain yield and water productivity in the irrigated sub-humid region of China. *Agric. Water Manag.* **2020**, *231*, 105935. [CrossRef]
10. Zhang, G.X.; Mo, F.; Shah, F.; Meng, W.H.; Liao, Y.C.; Han, J. Ridge-furrow configuration significantly improves soil water availability, crop water use efficiency, and grain yield in dryland agroecosystems of the Loess Plateau. *Agric. Water Manag.* **2021**, *245*, 106657. [CrossRef]
11. Prasad, J.K.; Dillip, K.S.; Suhas, P.W. Developing climate change agro-adaptation strategies through field experiments and simulation analyses for sustainable sorghum production in semi-arid tropics of India. *Agric. Water Manag.* **2023**, *286*, 108399.
12. Du, X.B.; He, W.C.; Wang, Z.; Xi, M.; Xu, Y.Z.; Wu, W.G.; Gao, S.Q.; Liu, D.; Lei, W.X.; Kong, L.C. Raised bed planting reduces waterlogging and increases yield in wheat following rice. *Field Crops Res.* **2021**, *265*, 108119. [CrossRef]
13. Liu, J.M.; Si, Z.Y.; Wu, L.F.; Shen, X.J.; Gao, Y.; Duan, A.W. High-low seedbed cultivation drives the efficient utilization of key production resources and the improvement of wheat productivity in the North China Plain. *Agric. Water Manag.* **2023**, *285*, 108357. [CrossRef]
14. Zhang, G.X.; Dai, R.C.; Ma, W.Z.; Fan, H.Z.; Meng, W.H.; Han, J.; Liao, Y.C. Optimizing the ridge-furrow ratio and nitrogen application rate can increase the grain yield and water use efficiency of rain-fed spring maize in the Loess Plateau region of China. *Agric. Water Manag.* **2022**, *262*, 107430. [CrossRef]
15. Wu, G.; Ling, J.; Liu, Z.X.; Xu, Y.P.; Chen, X.M.; Wen, Y.; Zhou, S.L. Soil warming and straw return impacts on winter wheat phenology, photosynthesis, root growth, and grain yield in the North China Plain. *Field Crops Res.* **2022**, *283*, 108545. [CrossRef]
16. Chang, T.G.; Shi, Z.; Zhao, H.L.; Song, Q.F.; He, Z.H.; Jeroen, V.R.; Bart, D.B.; Alexander, G.; Zhu, X.G. 3dCAP-Wheat: An Open-Source Comprehensive Computational Framework Precisely Quantifies Wheat Foliar, Nonfoliar, and Canopy Photosynthesis. *Plant Phenomics* **2022**, *97*, 58148. [CrossRef]
17. Gao, Y.M.; Zhang, M.; Yao, C.S.; Liu, Y.Q.; Wang, Z.M.; Zhang, Y.H. Increasing seeding density under limited irrigation improves crop yield and water productivity of winter wheat by constructing a reasonable population architecture. *Agric. Water Manag.* **2021**, *253*, 106951. [CrossRef]
18. Liu, F.S.; Song, Q.F.; Zhao, J.K.; Mao, L.X.; Bu, H.Y.; Hu, Y.; Zhu, X.G. Canopy occupation volume as an indicator of canopy photosynthetic capacity. *New Phytol.* **2021**, *232*, 941–956. [CrossRef]
19. Shahzad, A.; Xu, Y.Y.; Irshad, A.; Jia, Q.M.; Ma, X.C.; Amir, S.; Manzoor; Muhammad, A.; Ren, X.L.; Cai, T.; et al. The ridge-furrow system combined with supplemental irrigation strategies to improves radiation use efficiency and winter wheat productivity in semi-arid regions of China. *Agric. Water Manag.* **2019**, *213*, 76–86.
20. Jo, S.G.; Kang, Y.I.; Om, K.S.; Cha, Y.H.; Ri, S.Y. Growth, photosynthesis and yield of soybean in ridge-furrow intercropping system of soybean and flax. *Field Crops Res.* **2022**, *275*, 108329. [CrossRef]
21. Dong, W.L.; Yu, H.; Zhang, L.Z.; Wang, R.N.; Wang, Q.; Xue, Q.W.; Pan, Z.H.; Sun, Z.G.; Pan, X.B. Asymmetric Ridge-Furrow and Film Cover Improves Plant Morphological Traits and Light Utilization in Rain-Fed Maize. *J. Meteorol. Res.* **2018**, *32*, 829–838. [CrossRef]
22. Dai, Y.L.; Fan, J.L.; Liao, Z.Q.; Zhang, C.; Yu, J.; Feng, H.L.; Zhang, F.C.; Li, Z.J. Supplemental irrigation and modified plant density improved photosynthesis, grain yield and water productivity of winter wheat under ridge-furrow mulching. *Agric. Water Manag.* **2022**, *274*, 107985. [CrossRef]
23. Du, X.B.; Wang, Z.; Xi, M.; Wu, W.G.; Wei, Z.; Xu, Y.Z.; Zhou, Y.J.; Lei, W.X.; Kong, L.C. A novel planting pattern increases the grain yield of wheat after rice cultivation by improving radiation resource utilization. *Agric. For. Meteorol.* **2021**, *310*, 108625. [CrossRef]

24. Han, Y.j.; Wang, Y.C.; Zhang, D.M.; Gao, H.; Sun, Y.; Tao, B.; Zhang, F.Y.; Ma, H.; Liu, X.M.; Ren, H.L. Planting models and deficit irrigation strategies to improve radiation use efficiency, dry matter translocation and winter wheat productivity under semi-arid regions. *J. Plant Physiol.* **2023**, *280*, 153864. [CrossRef] [PubMed]
25. Liu, T.N.; Chen, J.Z.; Wang, Z.Y.; Wu, X.R.; Wu, X.C.; Ding, R.X.; Han, Q.F.; Cai, T.; Jia, Z.K. Ridge and furrow planting pattern optimizes canopy structure of summer maize and obtains higher grain yield. *Field Crops Res.* **2018**, *219*, 242–249. [CrossRef]
26. Liu, P.; Wang, H.l.; Li, L.C.; Liu, X.L.; Qian, R.; Wang, J.J.; Yan, X.Q.; Cai, T.; Zhang, P.; Jia, Z.K.; et al. Ridge-furrow mulching system regulates hydrothermal conditions to promote maize yield and efficient water use in rainfed farming area. *Agric. Water Manag.* **2020**, *232*, 106041. [CrossRef]
27. Si, Z.Y.; Liu, J.M.; Wu, L.F.; Li, S.; Wang, G.S.; Yu, J.C.; Gao, Y.; Duan, A.W. A high-yield and high-efficiency cultivation pattern of winter wheat in North China Plain: High-low seedbed cultivation. *Field Crops Res.* **2023**, *300*, 109010. [CrossRef]
28. Han, Y.Y.; Wang, Y.G.; Zhou, B.X.; Chen, Y.H.; Liu, P. Radiation use efficiency and yield response of winter wheat to planting patterns and irrigation in Northern China. *Agron. J.* **2014**, *106*, 168–174. [CrossRef]
29. Shahzad, A.; Xu, Y.Y.; Jia, Q.M.; Ma, X.C.; Irshad, A.; Muhammad, A.; Rushingabigwi, G.; Ren, X.L.; Zhang, P.; Cai, T.; et al. Interactive effects of plastic film mulching with supplemental irrigation on winter wheat photosynthesis, chlorophyll fluorescence and yield under simulated precipitation conditions. *Agric. Water Manag.* **2018**, *207*, 1–14.
30. Fan, Y.H.; Lv, Z.Y.; Qin, B.Y.; Yang, J.H.; Ren, K.M.; Liu, Q.X.; Jiang, F.Y.; Zhang, W.J.; Ma, S.Y.; Ma, C.X.; et al. Night warming at the vegetative stage improves pre-anthesis photosynthesis and plant productivity involved in grain yield of winter wheat. *Plant Physiol. Biochem.* **2022**, *186*, 19–30. [CrossRef]
31. Nader, M.O. An improved weighted average simulation approach for solving reliability-based analysis and design optimization problems. *Struct. Saf.* **2016**, *60*, 47–55.
32. Liu, P.J.; Zhang, T.; Zhang, F.Y.; Ren, X.L.; Chen, X.L.; Zhao, X.N. Ridge cropping and furrow irrigation pattern improved spring maize (*Zea mays* L.) yield and water productivity in Hetao irrigation area of Northwestern China. *J. Sci. Food Agric.* **2022**, *102*, 6889–6898. [CrossRef] [PubMed]
33. Cui, Z.J.; Gao, Y.H.; Guo, L.Z.; Wu, B.; Yan, B.; Wang, Y.F.; Liu, H.S.; Li, G.; Wang, Y.Z.; Wang, H.D. Optimal effects of combined application of nitrate and ammonium nitrogen fertilizers with a ratio of 3:1 on grain yield and water use efficiency of maize sowed in ridge-furrow plastic film mulching in Northwest China. *Agronomy* **2022**, *12*, 2943. [CrossRef]
34. Qiang, S.C.; Zhang, Y.; Fan, J.L.; Zhang, F.C.; Sun, M.; Gao, Z.Q. Combined effects of ridge-furrow ratio and urea type on grain yield and water productivity of rainfed winter wheat on the Loess Plateau of China. *Agric. Water Manag.* **2022**, *261*, 107340. [CrossRef]
35. Li, W.W.; Xiong, L.; Wang, C.J.; Liao, Y.C.; Wu, W. Optimized ridge-furrow with plastic film mulching system to use precipitation efficiently for winter wheat production in dry semi-humid areas. *Agric. Water Manag.* **2019**, *218*, 211–221. [CrossRef]
36. Du, X.B.; Wei, Z.; Kong, L.C.; Zhang, L.G. Optimal bed width for wheat following rice production with raised-bed planting in the Yangtze River Plain of China. *Agric. Water Manag.* **2022**, *269*, 107676. [CrossRef]
37. Luo, C.L.; Zhang, X.F.; Duan, H.X.; Zhou, R.; Mo, F.; Mburu, D.M.; Wang, B.Z.; Wang, W.; Kavagi, L.; Xiong, Y.C. Responses of rainfed wheat productivity to varying ridge-furrow size and ratio in semiarid eastern African Plateau. *Agric. Water Manag.* **2021**, *249*, 106813. [CrossRef]
38. Du, X.B.; Xi, M.; Wei, Z.; Chen, X.F.; Wu, W.G.; Kong, L.C. Raised bed planting promotes grain number per spike in wheat grown after rice by improving spike differentiation and enhancing photosynthetic capacity. *J. Integr. Agric.* **2023**, *22*, 1631–1644. [CrossRef]
39. Zhang, X.D.; Kamran, M.; Xue, X.K.; Zhao, J.; Cai, T.; Jia, Z.K.; Zhang, P.; Han, Q.F. Ridge-furrow mulching system drives the efficient utilization of key production resources and the improvement of maize productivity in the Loess Plateau of China. *Soil Tillage Res.* **2019**, *190*, 10–21. [CrossRef]
40. Zheng, H.Y.; Wang, J.Y.; Cui, Y.; Guan, Z.Y.; Yang, L.; Tang, Q.Q.; Sun, Y.F.; Yang, H.S.; Wen, X.Q.; Mei, N.; et al. Effects of Row Spacing and Planting Pattern on Photosynthesis, Chlorophyll Fluorescence, and Related Enzyme Activities of Maize Ear Leaf in Maize-Soybean Intercropping. *Agronomy* **2022**, *12*, 2503. [CrossRef]
41. Ma, S.T.; Mei, F.J.; Wang, T.C.; Liu, Z.D.; Ma, S.C. Stereoscopic Planting in Ridge and Furrow Increases Grain Yield of Maize (Zea mays L.) by Reducing the Plant's Competition for Water and Light Resources. *Agriculture* **2021**, *12*, 20. [CrossRef]
42. Ru, C.; Wang, K.F.; Hu, X.T.; Chen, D.Y.; Wang, W.E.; Yang, H.S. Nitrogen Modulates the Effects of Heat, Drought, and Combined Stresses on Photosynthesis, Antioxidant Capacity, Cell Osmoregulation, and Grain Yield in Winter Wheat. *J. Plant Growth Regul.* **2022**, *42*, 1681–1703. [CrossRef]
43. Ren, X.-L.; Zhang, P.; Chen, X.-L.; Jia, Z.-K. Impacts of ridge-furrow rainfall concentration systems and mulches on corn growth and yield in the semiarid region of China. *J. Sci. Food Agric.* **2016**, *96*, 3882–3889. [CrossRef] [PubMed]
44. Fang, H.; Liu, F.L.; Gu, X.B.; Chen, P.P.; Li, Y.P.; Li, Y.N. The effect of source-sink on yield and water use of winter wheat under ridge-furrow with film mulching and nitrogen fertilization. *Agric. Water Manag.* **2022**, *267*, 107616. [CrossRef]

45. Liu, X.L.; Wang, Y.D.; Yan, X.Q.; Hou, H.Z.; Liu, P.; Cai, T.; Zhang, P.; Jia, Z.K.; Ren, X.L.; Chen, X.L. Appropriate ridge-furrow ratio can enhance crop production and resource use efficiency by improving soil moisture and thermal condition in a semi-arid region. *Agric. Water Manag.* **2020**, *240*, 106289. [CrossRef]
46. Zhao, W.H.; Liu, L.Z.; Shen, Q.; Yang, J.H.; Han, X.Y.; Tian, F.; Wu, J.J. Effects of Water Stress on Photosynthesis, Yield, and Water Use Efficiency in Winter Wheat. *Water* **2020**, *12*, 2127. [CrossRef]